Science of the Total Environment 545–546 (2016) 465–475

Contents lists available at ScienceDirect

Science of the Total Environment

journal homepage: www.elsevier.com/locate/scitotenv

Stomatal uptake of O_3 in a *Schima superba* plantation in subtropical China derived from sap flow measurements

Junfeng Niu [a,b], Ping Zhao [a,b,*], Zhenwei Sun [a], Liwei Zhu [a,b], Guangyan Ni [a,b], Xiaoping Zeng [a], Zhenzhen Zhang [a,b], Xiuhua Zhao [a,b], Peiqiang Zhao [a,b], Jianguo Gao [a,b], Yanting Hu [a,b], Xiaomin Zeng [a,b], Lei Ouyang [a,b]

[a] Key Laboratory of Vegetation Restoration and Management of Degraded Ecosystems, South China Botanical Garden, Chinese Academy of Sciences, Xingke Road 523, Tianhe District, Guangzhou 510650, China
[b] Guangdong Provincial Key Laboratory of Applied Botany, South China Botanical Garden, Chinese Academy of Sciences, Xingke Road 523, Tianhe District, Guangzhou 510650, China

HIGHLIGHTS

- Canopy stomatal O_3 flux was derived from sap flow in a *Schima superba* plantation.
- Monthly integrated O_3 flux and exposure peaked in July and October, respectively.
- Accumulated O_3 flux exceeded the critical level for potential O_3 injury for trees.

GRAPHICAL ABSTRACT

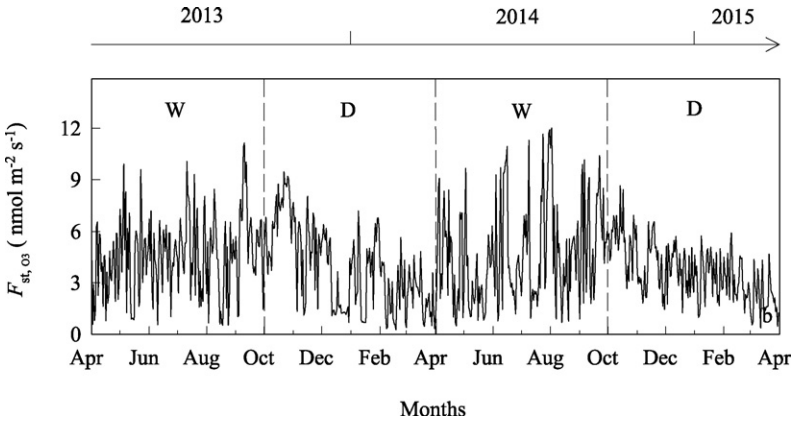

Dynamics of daily mean stomatal O_3 flux ($F_{st,O3}$) in a *Schima superba* plantation in subtropical China from April 2013 to March 2015 (D: dry seasons; W: wet seasons).

ARTICLE INFO

Article history:
Received 2 October 2015
Received in revised form 23 December 2015
Accepted 23 December 2015
Available online 4 January 2016

Editor: J. P. Bennett

Keywords:
Schima superba
Sap flow
Stomatal conductance
Ozone uptake
Risk assessment

ABSTRACT

Canopy stomatal ozone (O_3) flux ($F_{st,O3}$) in a plantation of *Schima superba*, an ecologically and economically important evergreen pioneer tree species in subtropical China, was quantified based on sap flow measurements during a 2-year period. Mean $F_{st,O3}$ and accumulated $F_{st,O3}$ ($AF_{st}0$) were significantly higher in wet seasons from April to September (4.62 nmol m^{-2} s^{-1} and 35.37 mmol m^{-2}, respectively) than in dry seasons from October to March (3.90 nmol m^{-2} s^{-1} and 24.15 mmol m^{-1}, respectively), yet comparable between the 2 years of the experiment, being 4.23 nmol m^{-2} s^{-1} and 58.23 mmol m^{-2} in April 2013–March 2014 and 4.29 nmol m^{-2} s^{-1} and 60.80 mmol m^{-2} in April 2014–March 2015, respectively. At the diurnal scale, $F_{st,O3}$ generally peaked in the early to middle afternoon hours (13:00–15:00), while the maximum stomatal conductance ($G_{st,O3}$) typically occurred in the middle to late morning hours (09:00–11:00). Monthly integrated $AF_{st}0$ reached the maximum in July, although accumulated O_3 exposure (*SUM*0) was highest in October. Seasonally or yearly, the accumulated O_3 doses, either exposure-based or flux-based, notably exceeded the currently adopted critical thresholds for the protection of forest trees. These results, on the one hand, demonstrated the decoupling between the stomatal uptake of O_3 and its environmental exposure level; on the other hand, indicated the potential O_3 risk for *S. superba* in the

* Corresponding author at: Key Laboratory of Vegetation Restoration and Management of Degraded Ecosystems, South China Botanical Garden, Chinese Academy of Sciences, Xingke Road 523, Tianhe District, Guangzhou 510650, China.
E-mail address: zhaoping@scib.ac.cn (P. Zhao).

http://dx.doi.org/10.1016/j.scitotenv.2015.12.122

experimental site. Therefore, the present study endorses the use of sap flow measurements as a feasible tool for estimating $F_{st,O3}$, and the transition from the exposure-based toward flux-based metrics for assessing O_3 risk for forest trees. Further studies are urgently needed to relate stomatal O_3 uptake doses with tree growth reductions for an improved understanding of O_3 effects on trees under natural conditions.

1. Introduction

Tropospheric ozone (O_3) is the most important air pollutant that may detrimentally affect tree growth and forest carbon sequestration under the global change scenarios (McLaughlin et al., 2007; Sitch et al., 2007). Atmospheric concentration of O_3 ([O_3]) in the Northern Hemisphere has increased from about 10 nmol mol^{-1} to currently between 20 and 45 nmol mol^{-1} since the pre-industrial era (Logan et al., 2012; Wittig et al., 2009), posing a substantial threat to forests in temperate and boreal regions (Fares et al., 2013b; Grulke et al., 2002; Matyssek et al., 2010). Background [O_3] is projected to continue to rise at a rate of 0.5–2.0% per year by the middle of this century (Fowler et al., 2008), although peak [O_3] in North America and Europe has leveled off or even decreased in recent decades (van Goethem et al., 2013). East Asia has also witnessed soaring surface [O_3] with its increasing emissions of nitrogen oxides (NO_x) and volatile organic compounds (VOCs), being as the O_3 precursors, and is expected to become a new hot spot area that would suffer from the highest [O_3] in the world in the coming decades, which may compromise present and future ecosystem services provided by regional forests (Itahashi et al., 2013; Lee et al., 2015). Thus it is urgently necessary to assess O_3 risk for forests in East Asia.

Two classes of metrics have been developed for O_3 risk assessment for tree species based on: (1) plant exposure to O_3, and (2) O_3 flux or uptake into plants (Fares et al., 2010a; Matyssek et al., 2004). [O_3] and its cumulative value, exposure (E) have been widely used and remain the basis for air quality standards in North America (US EPA, 2013). However, [O_3] and E reflect only the oxidative potential of the nearby air, which is different from the in situ O_3 stress experienced by the internal tissue of plants (Matyssek et al., 2008; Paoletti and Manning, 2007). More and more evidence suggests that the stomatal O_3 flux ($F_{st,O3}$), or the accumulated $F_{st,O3}$ over a threshold of Y ($AF_{st}Y$) be superior by taking into account the physiological and meteorological factors that may influence the actual doses of O_3 entering leaves and oxidizing apoplasts (Mills et al., 2010, 2011). The exposure-based methodology should therefore be replaced by the flux concept in the long run. Indeed, $F_{st,O3}$ has been quantified in a variety of tree species such as *Betula pendula*, *Fagus sylvatica* and *Picea abies*, and $AF_{st}Y$ has been used for O_3 risk assessment across Europe (Karlsson et al., 2007; Mills et al., 2011). However, $F_{st,O3}$ is still scant for trees species in East Asia, preventing the development of regionally specific critical levels (*CLs*) for forest protection.

$F_{st,O3}$ can be simulated by stomatal conductance (G_{st}) models (Emberson et al., 2000; Kinose et al., 2014), or measured directly by eddy covariance techniques (Kitao et al., 2014; Tuzet et al., 2011). The former depends on gas exchange measurements on enclosed leaves, and thus has the potential to disturb the boundary layers that counteract O_3 uptake (Matyssek et al., 2008); while the latter typically obtain total deposition, and stomatal O_3 uptake can hardly be separated from non-stomatal absorption onto plant and soil surfaces (Fares et al., 2014). According to the close coupling between transpiration and O_3 influx into leaves through stomata, $F_{st,O3}$ can be derived from sap flow measurements at tree trunks (Matyssek et al., 2015; Nunn et al., 2008, 2010; Wieser et al., 2003, 2006). This eco-physiological approach inherently accounts for the boundary layer effects, and has the advantage of being applicable in heterogeneous and mountainous landscapes, where eddy covariance methods may fail (Nunn et al., 2008). However, sap flow-based derivation of $F_{st,O3}$ can be highly biased because of technical and meteorological reasons (Ewers and Oren, 2000), which should be addressed sufficiently if credible results are to be obtained.

In the Pearl River Delta (PRD) of South China, due to the rapid industrialization and urbanization, ground [O_3] has increased and become one of the primary environmental concerns, causing significant reductions in crop yields (Tang et al., 2013, 2014). However, to our knowledge, there is not any study that has been conducted to examine the potential impact of O_3 on the native tree species in this region, particularly from the perspective of stomatal O_3 flux or uptake. In consideration of the peculiarities in climate, tree physiology and phenology, dynamic patterns of $F_{st,O3}$ should be unique in this region. Here, we selected a plantation of *Schima superba*, an ecologically and economically important pioneer tree species in PRD, and quantified its $F_{st,O3}$ at the stand level based on sap flow measurements during a 2-year period. We hypothesize that (1) $F_{st,O3}$ in *S. superba* is comparable to those reported in temperate and Mediterranean species, while its dynamic features may be unique, (2) decoupling exists between the exposure-based and flux-based metrics for *S. superba* and (3) the currently adopted *CLs* for the protection of forest trees have been exceeded, and *S. superba* may potentially be stressed by O_3 in our experimental site. The results would contribute to a more scientific O_3 risk evaluation for regional forest trees.

2. Materials and methods

2.1. Site description

The study was performed at the Xiaoqingshan ecological observation station in a pure plantation (2885 m^2) of 35- to 40-year-old *S. superba* grown at a northeastern slope with an inclination of 11.7° within South China Botanical Garden, Chinese Academy of Sciences, Guangzhou, China (23°10′48″ N, 113°21′04″ E). It has a typical subtropical oceanic monsoon climate, characterized by a hot, humid season from April to September (wet season), and a warm, dry season from October to March (dry season). Long-term average of annual air temperature (T) from 1971 to 2014 was 22.1 °C, with July and January as the hottest (28.6 °C) and coldest (13.5 °C) months, respectively. Average annual precipitation (P) was 1770.3 mm, with more than 80% concentrating on wet seasons (http://www.escience.gov.cn/metdata/page/index.html). The soil is a gravely sandy loam with pH of 4.0–5.0, organic content of 2.3% and total nitrogen content of 0.07%. The plantation had developed a closed canopy at the height of between 10–13 m above the ground, with the leaf area index (*LAI*) varying from 3.3 m^2 m^{-2} in February to 4.9 m^2 m^{-2} in May (Fig. 1). Understory plants are sparse, and tree density, basal stem area and average diameter at the breast height (*DBH*) were 1246 trees ha^{-1}, 29.8 m^2 ha^{-1} and 16.4 cm, respectively.

2.2. Measurements

2.2.1. Stand LAI and tree samples

LAI of the plantation was measured monthly from 2009 to 2014 with a *LAI*-2000 plant canopy analyzer (LI-COR, Inc., Lincoln, NE, USA). *DBH*s were gauged for all trees in June 2014. Each tree was grouped into one of the following *DBH* classes: I (*DBH* ≤ 15 cm), II (15 cm < *DBH* ≤ 25 cm) and III (*DBH* > 25 cm), and trees within the *DBH* classes I, II and III accounted for 43.15%, 49.24% and 7.61% of the total trees of the whole plantation, respectively. 21 trees (5, 12 and 4 trees for the *DBH* classes

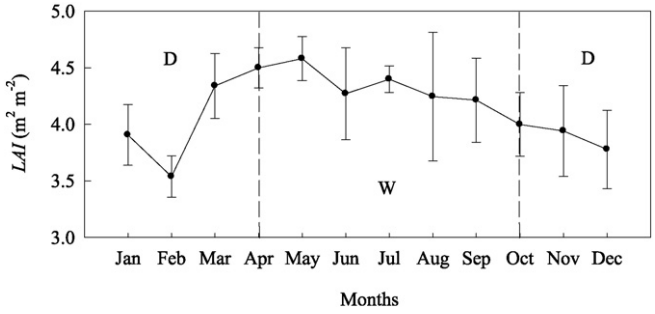

Fig. 1. Monthly dynamics of the leaf area index (*LAI*) at the *Schima superba* plantation from 2009 to 2014 (n = 6, and vertical bars represent ± 1 standard deviation. D: dry seasons; W: wet seasons).

I, II and III, respectively) were sampled and used for sap flow measurements. In another 16 trees (5, 8 and 3 trees for the *DBH* classes I, II and III, respectively), depth of sapwood (D_s) was determined by a distinct color change between sapwood and heartwood in increment cores, and the following allometric relationship ($r^2 = 0.99$, $p < 0.01$) was established:

$$A_s = 0.6841 \times DBH^2.0226 \quad (1)$$

Eq. (1) was then used to derive sapwood area (A_s) for all individual trees based on their *DBH*s. Other biometric parameters including tree height (H_t), bole height (H_b), crown height (H_c) and crown area (A_c) were also measured or calculated for the 21 trees that were sampled for sap flow measurements. H_t and H_b were measured with a Trupulse 200L laser rangefinder (Laser Technology, Inc., Colorado, USA), H_c was calculated as ($H_t - H_b$), and A_c was estimated as the ellipse area with two perpendicular crown diameters (one was the largest crown diameter) as the major and minor axes, respectively (Table 1).

2.2.2. Sap flow

Sap flux density (J_s) was measured by home-made thermal dissipation probes (TDPs). Two probes, 20 mm in length and 1.1 mm in diameter, were radially inserted, 15 cm apart, into tree stems. The downstream probes, positioned at the upper part of the stem, were constantly heated at 0.2 W, while the upstream probes, positioned at the lower part of the stem, were unheated. Temperature differences between the two probes (ΔT) were sensed by the copper–constantan thermocouple located at the middle of the heated probe, and converted to J_s by the empirical formula suggested by Granier (1987):

$$J_s = 119 \times [(\Delta T_{max} - \Delta T)/\Delta T]^1.231 \quad (2)$$

where ΔT_{max} is the ΔT under zero flow conditions, and was determined when (a) *VPD* < 0.05 kPa over a 2-hour period, and thus nocturnal transpiration was negligible, and (b) ΔT_{max} was stable over a 2-hour period, so it was impossible for nocturnal stem water recharge (Oishi et al., 2008). Sensor outputs were collected every 30 s, averaged over 10 min and recorded with a *DL2e* data logger (Delta-T Devices Ltd., Cambridge, UK). All sensors were installed at the breast height (1.3 m above the ground), and wrapped in aluminum foil to prevent solar heating.

Table 1
Means of the diameter at the breast height (*DBH*), tree height (H_t), bole height (H_b), crown height (H_c), crown area (A_c), sapwood depth (D_s) and sapwood area (A_s) for the *Schima superba* trees sampled for sap flow measurements (Mean ± SD, n = 21).

DBH (cm)	H_t (m)	H_b (m)	H_c (m)	A_c (m^2)	D_s (cm)	A_s (cm^2)
20.3 ± 6.3	12.2 ± 0.8	10.1 ± 0.6	2.1 ± 0.3	13.4 ± 8.3	6.1 ± 2.0	297.6 ± 182.8

2.2.3. [O_3]

[O_3] was monitored outside the plantation as a composite item of a comprehensive project for monitoring air pollutants including SO_2, NOx and O_3. The whole platform was placed in a building room (at the 5th floor and 10 m above the ground) that was horizontally 100 m away from the plantation. Atmospheric air was constantly pumped from a height of 13.2 m (above the ground), through a 6 m Teflon tube, into a UV-absorption analyzer (Model 49*i*, Thermo Fisher Scientific Inc., MA, USA) for real-time [O_3] detection. Alternative sampling analyses prior to the experiment detected no significant differences ($p > 0.1$) in [O_3] between the monitoring site and other sites (5 sites were analyzed) of the same height (13.2 m above the ground) just above the plantation canopy, and thus confirmed the validity of our measurements. Calibrations for the Model 49*i* were carried out based upon the US EPA approved procedure using a UV photometer as a calibration standard at a weekly basis. A Model 146*i* Multi-gas calibrator (Thermo Fisher Scientific Inc., MA, USA) was used to dilute the standard gas (20 μmol mol^{-1}) (Beijing AP BAIF Gases Industry Co., Ltd., Beijing, China) to precise concentrations. Every year, both Model 49*i* and Model 146*i* were sent back to the manufacturer for regular maintenance and calibration. [O_3] was detected every 30 s, averaged over 10 min as an output record, then averaged over 60 min as the hourly mean [O_3] ($[O_3]_h$). *SUM*0 and *SUM*60 were calculated as sum of $[O_3]_h$ and sum of $[O_3]_h$ when $[O_3]_h \geq 60$ nmol mol^{-1}, respectively. Accumulated O_3 exposure over a threshold of 40 nmol mol^{-1} (*AOT*40) was computed according to Eq. (3). Throughout the 2 years of the experiment, missing data accounted for 0.7% and were filled through linear interpolations.

$$AOT40 = \sum([O_3]_h - 40) \text{ when } [O_3]_h \geq 40 \text{ nmol mol}^{-1} \quad (3)$$

2.2.4. Micrometeorology

Photosynthetically active radiation (*PAR*) was quantified with a *LI*-190SA quantum sensor (LI-COR, Inc., Lincoln, NE, USA), and the horizontal wind speed (u) was measured by an AN4 standard anemometer (Delta-T Devices Ltd., Cambridge, UK). T and relative air humidity (*RH*) were sensed at the canopy height by a thermo-hygrometer (HygroClip 2, Rotronic AG, Switzerland), and vapor pressure deficit (*VPD*) was calculated from T and *RH* according to Campbell and Norman (1998). Soil water content (*SWC*) at 30 cm depth was measured at 3 different locations with SM150 soil moisture sensors (Delta-T Devices Ltd., Cambridge, UK). P was recorded in a nearby meteorological station. All the sensors for meteorological measurements were deployed at the canopy height of 13.2 m (above the ground) and mounted on a 16.5 m high steel tower erected at the center of the plantation. All measurements were synchronized with J_s and lasted for 2 years from April 2013 to March 2015. Missing data for micrometeorology (4.2%) due to instrument malfunctions were filled by linear regressions with their corresponding values monitored at the nearby meteorological station.

2.3. Transpiration (E)

In the present study, all TDPs were in complete contact with the stem sapwood ($D_s > 20$ mm), and thus it was unnecessary to incur a correction for non-conductive tissues (Clearwater et al., 1999). Previous studies conducted in the same plantation detected no consistently circumferential variation in J_s (Zhou et al., 2012; Zhu et al., 2012), so J_s was measured uniformly on the northern sides of tree trunks. However, J_s was found to decrease significantly toward inner sapwood, being 45% lower at the >40 mm depth than at the ≤40 mm depth, and such radial variation was integrated according to Mei et al., 2010 and Zhu et al., 2012. Size-related variability in J_s among individual trees (Meinzer et al., 2001) was accounted for through the respective measurements of J_s for different *DBH* groups, as described in Section 2.2.2. Besides, in our *S. superba* plantation, tree sizes and thus sapwood volumes are

relatively small, therefore bole water contributes little to daily sap flow, rendering the potential time lags between E and J_s negligible (Zhao et al., 2013; Zhou et al., 2012). Based on these specifications, E for daytime hours could be credibly quantified as:

$$E = \sum (J_{si,\le 40\ mm} \times A_{si,\le 40\ mm} + J_{si,>40\ mm} \times A_{si,>40\ mm})/S \quad (4)$$

where $J_{si,\le 40\ mm}$ and $J_{si,>40\ mm}$ are the mean J_s at the stem depth of ≤40 mm and >40 mm for the *DBH* class i (i = I, II or III), and $J_{si,>40\ mm}$ is quantified as $0.55 \times J_{si,\le 40\ mm}$. $A_{si,\le 40\ mm}$ and $A_{si,>40\ mm}$ are the corresponding A_s for $J_{si,\le 40\ mm}$ and $J_{si,>40\ mm}$, respectively. S represents the plantation area.

2.4. Canopy stomatal conductance to water vapor ($G_{st,H2O}$)

$G_{st,H2O}$ was estimated from E according to Eq. (5) (Montheith and Unsworth, 1990) when J_s was available for at least three trees in each *DBH* class. Such data accounted for 64.5% and 71.3% of the first and second years of the experiment, respectively.

$$G_{st,H2O} = (K \times E)/VPD \quad (5)$$

Where K is the conductance coefficient that accounts for the effects of T on psychrometric constant, latent heat of vaporization, and specific heat and density of air, and can be expressed as $115.8 + 0.4236 \times T$ (Phillips and Oren, 1998). Eq. (5) requires that the boundary layer conductance is high, and T and RH at the leaf surface are equal to their corresponding values in the within-canopy free atmosphere (Ewers and Oren, 2000). In our *S. superba* plantation, leaf sizes and densities are small, canopy surface is rough and winds are prevalent, therefore individual leaves should be well coupled with the surrounding air.

During periods when J_s was unavailable (19.5% and 13.9% for the first and second years of the experiment, respectively), or when low *VPD*

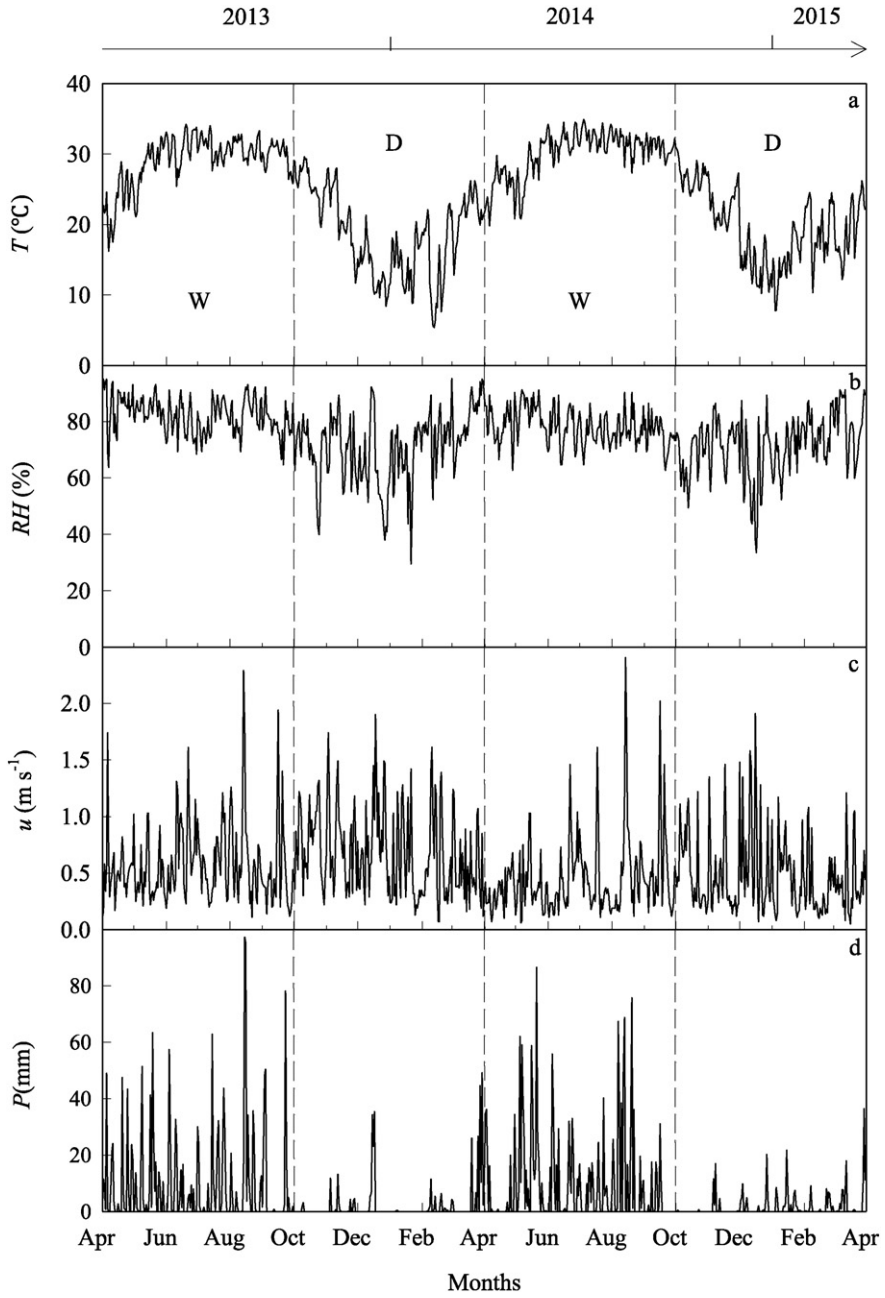

Fig. 2. Daily means (24 h) of air temperature (T) (a), relative air humidity (RH) (b), wind speed (u) (c) and daily total precipitation (P) (d) from April 2013 to March 2015 (D: dry seasons; W: wet seasons).

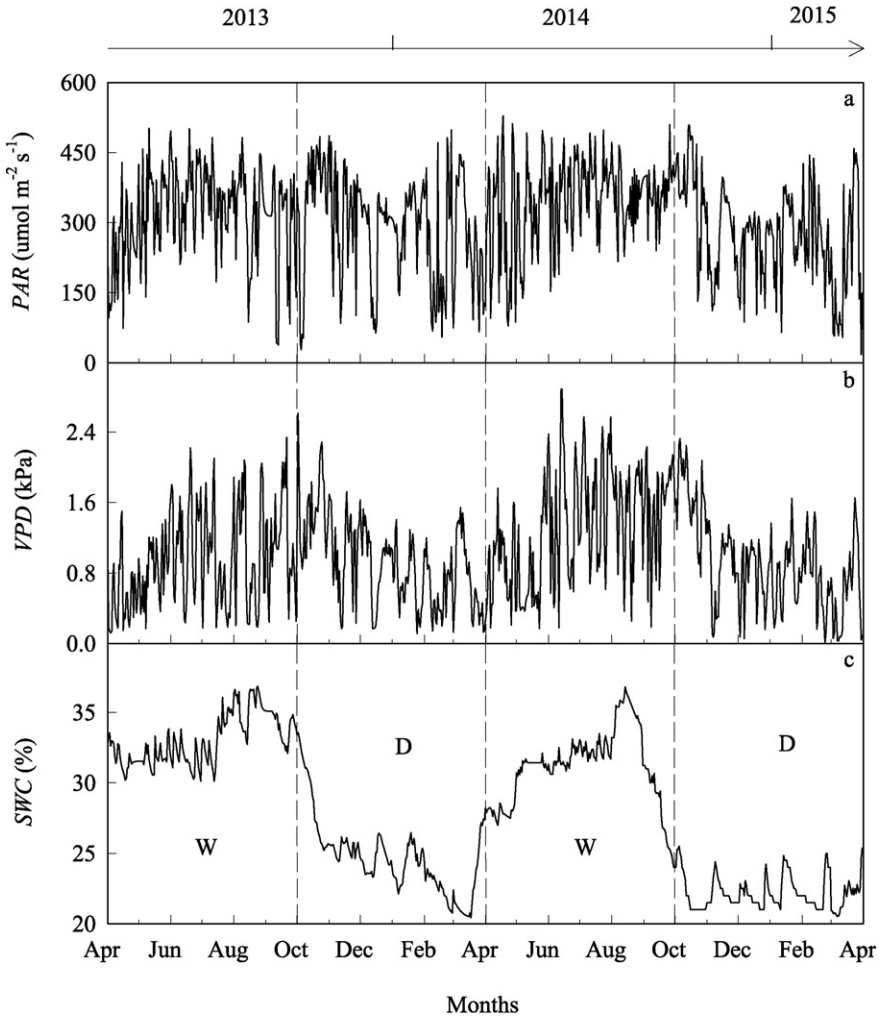

Fig. 3. Daily means of photosynthetically active radiation (*PAR*) (a), vapor pressure deficit (*VPD*) (b) and soil water content (*SWC*) (c) when photosynthetically active radiation (*PAR*) > 106 μmol m^{-2} s^{-1} from April 2013 to March 2015 (D: dry seasons; W: wet seasons).

(<0.6 kPa) caused large uncertainties (>10%) in using Eq. (5) (Ewers and Oren, 2000), $G_{st,H2O}$ was simulated by a multiplicative model with *PAR* and *VPD* as the predictor variables (Uddling et al., 2010):

$$G_{st,H2O} = G_{st,H2O}(VPD) \times f(PAR) \quad (6)$$

where $G_{st,H2O}(VPD)$ is the specific relationship between *VPD* and J_s-derived $G_{st,H2O}$ (Oren et al., 1999), and $f(PAR)$ is the relative response function between 0 and 1 for *PAR* (Feng et al., 2012). For *VPD* < 0.6 kPa, $G_{st,H2O}(VPD)$ was assumed to plateau at its value at *VPD* = 0.6 kPa ($G_{st,max}$) rather than to continue to increase with decreasing *VPD* (Uddling et al., 2010). *SWC* was not introduced into Eq. (6) because it was constantly higher than 20% in our experimental site, exceeding the potential threshold for significant inhibition on $G_{st,H2O}$ (Bell et al., 2015; Bueker et al., 2012). All *E* and $G_{st,H2O}$ were calculated as hourly averages, and expressed in per unit of projected leaf area (*PLA*), with daytime hours defined as *PAR* > 106 μmol m^{-2} s^{-1} according to UNECE (2004).

2.5. Canopy stomatal conductance to O_3 ($G_{st,O3}$) and $F_{st,O3}$

$G_{st,H2O}$ was converted into $G_{st,O3}$ by multiplying with 0.613, the ratio of the molecular diffusivities of O_3 to water vapor (Campbell and Norman, 1998). $F_{st,O3}$ was calculated according to Eq. (7), assuming that $[O_3]$ in the intercellular leaf space approaches zero (Laisk et al., 1989).

$$F_{st,O3} = G_{st,O3} \times [O_3] \quad (7)$$

Table 2
Values for the maximum G_{st} ($G_{st,max}$), *a*, *b* and *m* in $G_{st,H2O} = -m\ln(VPD) + b$ and $f(PAR) = 1 - \exp(-a \cdot PAR)$ during different growing seasons from April 2003 to March 2015 (dry seasons: October–March; wet seasons: April–September).

Parameters (units)	April 2013–March 2014		April 2014–March 2015	
	Wet season	Dry season	Wet season	Dry season
$G_{st,max}$ (mmol m^{-2} PLA s^{-1})	563.08 ± 3.56	502.72 ± 2.72	555.71 ± 2.57	504.12 ± 4.60
a (constant)	0.0020 ± 0.0002	0.0018 ± 0.0001	0.0018 ± 0.0002	0.0017 ± 0.0002
b (mmol m^{-2} s^{-1})	433.94 ± 5.88	403.68 ± 4.48	445.32 ± 4.64	400.06 ± 8.32
m (mmol m^{-2} s^{-1} ln(kPa)$^{-1}$)	252.80 ± 9.24	183.90 ± 7.09	216.10 ± 6.34	203.70 ± 11.61

Table 3
Regressions of sap flow-derived stomatal conductance to water vapor ($G_{st,H2O}$) to modeled $G_{st,H2O}$ during different growing seasons from April 2013 to March 2015 (Dry seasons: October–March; Wet seasons: April–September).

Durations	Equations	*df*	*F*	*p*	r^2_a	r^2_b	Errors
April 2013–March 2014							
Wet season	$y = 0.85x + 6.22$	(1,610)	893.13	<0.01	0.59	0.55	7.19 ± 0.08%
Dry season	$y = 0.81x + 6.69$	(1,1197)	2387.55	<0.01	0.67	0.62	4.38 ± 0.02%
April 2014–March 2015							
Wet season	$y = 0.95x + 6.89$	(1,477)	778.91	<0.01	0.62	0.60	−5.73 ± 0.05%
Dry season	$y = 0.99x + 2.38$	(1,1479)	3354.44	<0.01	0.69	0.69	−3.80 ± 0.01%

r^2_a: r^2 for linear regressions of sap flow-derived $G_{st,H2O}$ to modeled $G_{st,H2O}$; r^2_b: r^2 for the 1:1 relationships between sap flow-derived $G_{st,H2O}$ and modeled $G_{st,H2O}$. Positive/negative errors mean that $G_{st,H2O}$ was overestimated/underestimated.

Accumulated stomatal O_3 flux over a threshold of Y nmol m^{-2} s^{-1} ($AF_{st}Y$) was estimated by integrating positive values of ($F_{st,O3}-Y$), and compared to *AOT*40 for specific time periods,

$$AF_{st}Y = \sum (F_{st,O3} - Y) \text{ for } F_{st,O3} \geq Y \quad (8)$$

Y was set to 0, 1 and 1.6 nmol m^{-2} s^{-1} according to UNECE (2004) and Mills et al. (2011).

2.6. Statistical analyses

Raw data of TDPs were transformed into J_s with the Baseliner Program (Version 3.0.7, C-H_2O Ecology Lab, Duke University, Durham, NC, USA). Functional relationships of $G_{st,H2O}$ to *VPD* and *PAR* were established through boundary line analyses with an Excel Macro (Boundryliner, C-H_2O Ecology Lab, Duke University, Durham, NC, USA). Linear regressions were implemented to examine the consistency between J_s-derived and modeled $G_{st,H2O}$. Independent-Samples T-Tests were conducted to determine the significance of differences in micrometeorology, [O_3] and $F_{st,O3}$ between years and seasons (no interactions were found between years and seasons based on pre-analyses with two-way ANOVAs). All analyses were performed using SAS software (Version 9.1.3, SAS Institute, Cary, NC, USA), and considered significant if $p < 0.05$. Figures were graphed in Sigma Plot (*Version 12.1*, Systat Software Inc., CA, USA).

3. Results

Mean (24 h) *T* and *RH* were similar ($p > 0.05$) in April 2013–March 2014 (23.8 °C and 76.5%) and April 2014–March 2015 (24.9 °C and 76.9%). Across the 2 years of the experiment, mean (24 h) *T* and *RH* in

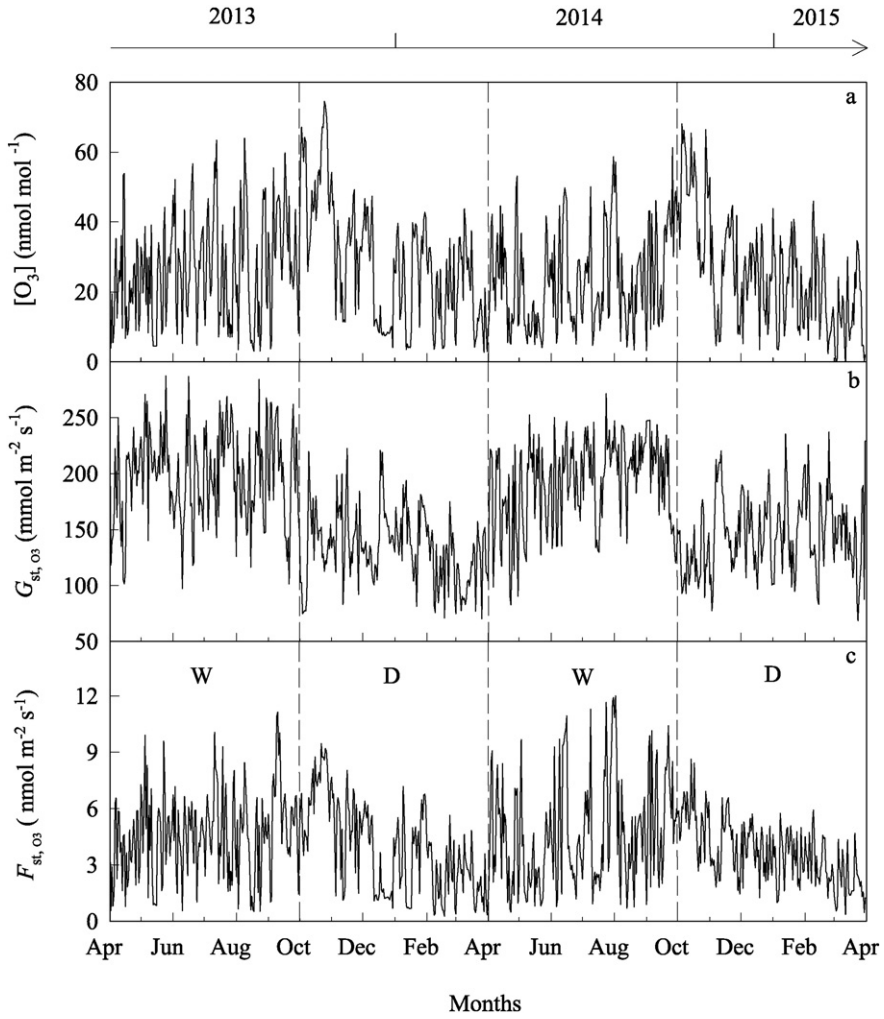

Fig. 4. Daily means of O_3 concentration [O_3] (a), canopy stomatal conductance to O_3 ($G_{st,O3}$) (b) and stomatal O_3 flux ($F_{st,O3}$) (c) when photosynthetically active radiation (*PAR*) > 106 μmol m^{-2} s^{-1} from April 2013 to March 2015 (D: dry seasons; W: wet seasons).

wet seasons (29.6 °C and 82.7%) were significantly higher than those in dry seasons (19.1 °C and 70.7%). In contrast, mean (24 h) *u* was significantly higher in dry seasons (0.58 m s^{-1}) than in wet seasons (0.51 m s^{-1}), and also in April 2013–March 2014 (0.63 m s^{-1}) than in April 2014–March 2015 (0.47 m s^{-1}). *P* was slightly lower ($p > 0.05$) in April 2013–March 2014 (2111.0 mm) than in April 2014–March 2015 (2143.6 mm), with 82.9% and 85.4% concentrating on wet seasons for the first and second years of the experiment, respectively (Fig. 2).

Mean (daytime hours) *PAR* was slightly lower in April 2013–March 2014 (395.1 μmol m^{-2} s^{-1}) than in April 2014–March 2015 (403.8 μmol m^{-2} s^{-1}), but higher in wet seasons (431.7 μmol m^{-2} s^{-1}) 1) than in dry seasons (367.0 μmol m^{-2} s^{-1}). However, neither of these two differences was significant due to lager standard deviations (97.0–117.4 μmol m^{-2} s^{-1}) of *PAR*. Mean (daytime hours) *VPD* and *SWC* were significantly higher in wet seasons (1.12 kPa and 32.2%) than in dry seasons (0.91 kPa and 25.8%). Mean (daytime hours) *VPD* was also significantly higher in April 2014–March 2015 (1.11 kPa) than in April 2013–March 2014 (0.93 kPa), but mean (daytime hours) *SWC* was comparable ($p > 0.05$) between the two years, being 28.9% and 26.7% in the first and second years of the experiment, respectively. Maximum daily average (daytime hours) *VPD* occurred in October (2.28 kPa) in 2013–March 2014, and in June (2.89 kPa) in April 2014–March 2015, while maximum daily average (daytime hours) *SWC* occurred in August for both years of the experiment (36.9% and 36.8% for the first and second years of the experiment, respectively) (Fig. 3).

The model used to simulate $G_{st,H2O}$ during periods when J_s was missing or *VPD* < 0.6 kPa was fitted for wet and dry seasons within each year, respectively, and the corresponding parameters were shown in Table 2. On average, $G_{st,max}$ and *b* were 11.1% and 9.4% higher in wet seasons than in dry seasons across the 2 years of the experiment. *m* and *a* were 37.5% and 11.1% higher in the wet season than in the dry season in April 2013–March 2014, while only 6.1% and 5.9% higher in the wet season than in the dry season in April 2014–March 2015. There were significant linear relationships between J_s-derived $G_{st,H2O}$ and modeled $G_{st,H2O}$ during the period when J_s was available (Table 3). The model explained on average 57.5% and 65.5% (r^2 of the 1:1 line) of the variation in J_s-derived $G_{st,H2O}$ for wet and dry seasons, respectively, being slightly lower than the mean r^2 of 60.5% and 68.0% for linear regressions of J_s-derived $G_{st,H2O}$ to modeled $G_{st,H2O}$. The model performed similarly in April 2014–March 2015 (mean r^2 = 65.5%) and April 2013–March 2014 (mean r^2 = 63.0%). In the first year of the experiment, $G_{st,H2O}$ was overestimated by 7.19% and 4.38% for the wet and dry seasons, respectively; however, it was underestimated in the second year by 5.73% and 3.80% for the wet and dry seasons, respectively (Table 3).

Mean (daytime hours) $[O_3]$ was significantly lower in wet seasons (25.12 nmol mol^{-1}) than in dry seasons (29.11 nmol mol^{-1}), yet comparable ($p > 0.05$) between April 2013–March 2014 (27.29 nmol mol^{-1}) and April 2014–March 2015 (26.93 nmol mol^{-1}). In contrast, mean (daytime hours) $G_{st,O3}$ was significantly higher in wet seasons (195.59 mmol m^{-2} s^{-1}) than in dry seasons (139.64 mmol m^{-2} s^{-1}), yet still comparable ($p > 0.05$) between April 2013–March 2014 (166.69 mmol m^{-2} s^{-1}) and April 2014–March 2015 (168.70 mmol m^{-2} s^{-1}). Similarly, mean (daytime hours) $F_{st,O3}$ was significantly higher in wet seasons (4.62 nmol m^{-2} s^{-1}) than in dry seasons (3.90 nmol m^{-2} s^{-1}), and slightly lower ($p > 0.05$) in April 2013–March 2014 (4.23 mmol m^{-2} s^{-1}) than in April 2014–March 2015 (4.29 mmol m^{-2} s^{-1}). Maximum daily average (daytime hours) $F_{st,O3}$ occurred in September (11.14 mmol m^{-2} s^{-1}) in April 2013–March 2014, and in August (12.01 mmol m^{-2} s^{-1}) in April 2014–March 2015, while maximum daily average (daytime hours) $[O_3]$ occurred in October for both years of the experiment (74.48 and 71.43 nmol mol^{-1} for the first and second years of the experiment, respectively) (Fig. 4).

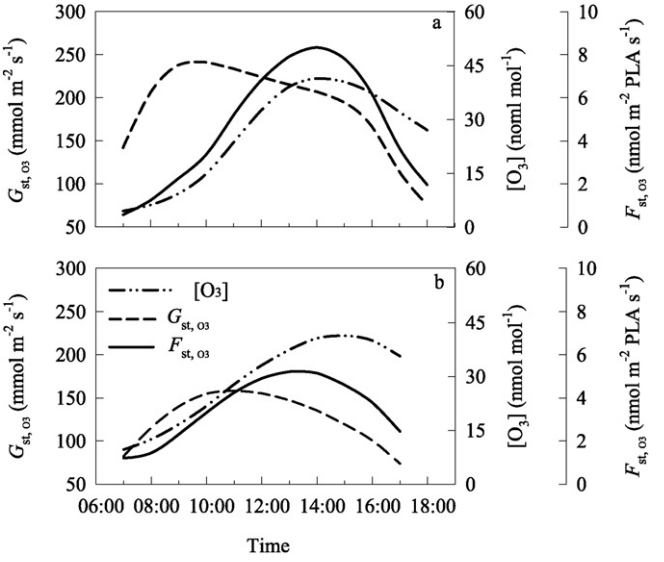

Fig. 5. Diurnal dynamics of canopy stomatal conductance to O_3 ($G_{st,O3}$), O_3 concentration ($[O_3]$), and stomatal O_3 flux ($F_{st,O3}$) for wet (a) and dry seasons (b) from April 2013 to March 2015.

4. Discussion

4.1. Comparisons with other studies

$F_{st,O3}$ and $AF_{st}Y$ in our *S. superba* plantation were comparable to those in other forest stands and trees estimated by either sap flow or models and eddy covariance techniques (Table 4). In a 53- to 60-year-old mixed evergreen and deciduous forest (*P. abies* and *F. sylvatica*), mean $F_{st,O3}$ during the period of 2–29 July 2007 was determined as 5.7 and 7.2 nmol m^{-2} s^{-1} based on sap flow and eddy covariance techniques,

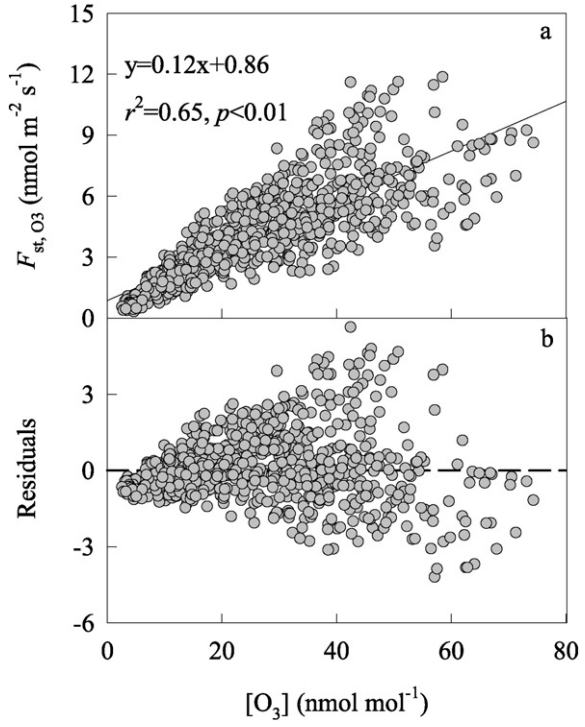

Fig. 6. Linear regression relationship of the daily average stomatal O_3 flux with ambient O_3 concentration ($[O_3]$) (a) and the regression residuals (b) for a *Schima superba* plantation from April 2013 to March 2015.

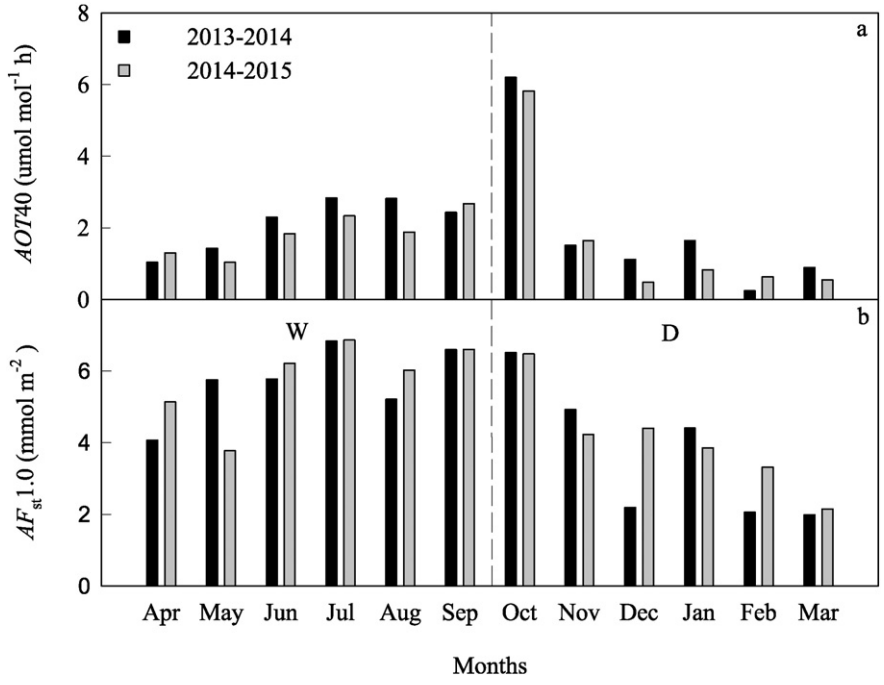

Fig. 7. Monthly integrated *AOT*40 (a) and $AF_{st}1.0$ (b) for daytime hours ($PAR > 106\ \mu mol\ m^{-2}\ s^{-1}$) from April 2013 to March 2015 in the *Schima superba* plantation (*AOT*40: accumulated O_3 exposure over a threshold of 40 nmol mol^{-1}; $AF_{st}1.0$: accumulated O3 flux over a threshold of 1.0 nmol $m^{-2}\ s^{-1}$; D: dry seasons; W: wet seasons).

respectively (Nunn et al., 2010), which agreed well with the average $F_{st,O3}$ of 6.2 nmol $m^{-2}\ s^{-1}$ in October in the present study. By simultaneously measuring the O_3 flux above and below the canopy of a 40- to 50-year-old Mediterranean evergreen forest (*Quercus ilex*), Fares et al. (2014) found that mean $F_{st,O3}$ ranged from 2.7 nmol $m^{-2}\ s^{-1}$ in the winter to 5.0 nmol $m^{-2}\ s^{-1}$ in the spring in 2013, which was also in line with the $F_{st,O3}$ in our *S. superba* plantation that ranged from 3.7 nmol $m^{-2}\ s^{-1}$ in dry seasons to 4.6 nmol $m^{-2}\ s^{-1}$ in wet seasons. During March–December 2004, $AF_{st}0$ in a 30-year-old mixed evergreen and deciduous forest (*Ilex pedunculosa* and *Quercus serrata*) was quantified as 51.8 mmol m^{-2} by the Penman–Monteith approach in combination with the Ball–Woodrow–Berry model (Kitao et al., 2014). Still, this result was fairly congruent with the yearly average $AF_{st}0$ of 59.5 mmol m^{-2} in *S. superba* in our present study, especially in consideration of the different time durations for $AF_{st}0$ calculation between these two studies. Similar $F_{st,O3}$ and $AF_{st}Y$ have also been reported in evergreen *Pinus cembra* and deciduous *Larix decidua*, *Aesculus chinensis* and *Magnolia liliiflora* (Wang et al., 2012; Wieser et al., 2003). Based on these comparisons, the present sap flow-derived $F_{st,O3}$ for *S. superba* should be highly credible.

4.2. Decoupling between ambient O_3 exposure and stomatal O_3 uptake

This study clearly illustrates the decoupling relationship between the exposure to and stomatal uptake of O_3 in the present *S. superba* plantation. Diurnally, maximum [O_3] occurred between 14:00 and 16:00 (Fig. 5), which agreed well with those observed in the "Castello" site (41°44′N, 12°24′E) (Fares et al., 2013a) and the University of Michigan Biological Station AmeriFlux (UMBS Flux) site (45°36′N, 84°43′W) (Seok et al., 2013), suggesting that O_3 accumulated in the boundary layer before being effectively removed during the late afternoon hours (Fares et al., 2014). By contrast, $G_{st,O3}$ peaked between 09:00 and 11:00, and declined due to high levels of *VPD* during the afternoon hours (Fig. 5), which was also in line with those found in a mixed forest of *P. abies* and *F. sylvatica* (Matyssek et al., 2015), and in pure forests of *P. abies*, *L. decidua* and *P. cembra* (Nunn et al., 2008). As a result, maximum $F_{st,O3}$ concurred with maximum [O_3] in wet seasons, but happened earlier than maximum [O_3] in dry seasons in (Fig. 5). Similar results have also been reported at the Kranzberger Forest (48°25′N, 11°39′E) (Matyssek et al., 2015; Nunn et al., 2010), and in a *Pinus ponderosa* stand at the Blodgett Ameriflux site (38°53′N, 120°37′W)

Table 4
Stomatal O_3 flux ($F_{st,O3}$) or uptake ($AF_{st}0$) in the present *Schima superba* plantation and in other forest stands and trees and in literature.

Species	Tree age (years)	$F_{st,O3}$ (nmol $m^{-2}\ s^{-1}$)	$AF_{st}0$ (mmol m^{-2})	Study duration	Study levels	Methods (SF/EC/M)[a]	References
S. superba	35–40	4.26	119.0	April 2013–March 2015	Stands	SF	Present study
M. liliiflora	~50	4.8	21.0	May–October 2009	Trees	SF	Wang et al. (2012)
A. chinensis	~50	4.0	19.2	May–October 2009	Trees	SF	Wang et al. (2012)
P. tremuloides	8–9	NA	36.9	June to August 2004 & 2005	Stands	SF	Uddling et al. (2010)
P. tremuloides & *B. papyrifera*	8–9	NA	32.7	June to August 2004 & 2005	Stands	SF	Uddling et al. (2010)
Q. ilex	40–50	3.9	NA	January–December 2013	Stands	EC	Fares et al. (2014)
Q. serrata & *I. pedunculosa*	~30	NA	51.8	March–December 2004	Stands	EC&M	Kitao et al. (2014)
F. sylvatica & *P. abies*	53–60	5.1&7.2	NA	2–29 July 2007	Stands	SF&EC	Nunn et al. (2010)
P. cembra	80–100	5.9	NA	28 April and 6 October 1998	Trees	SF	Wieser et al. (2003)
L. decidua	80–100	3.9	NA	28 April and 6 October 1998	Trees	SF	Wieser et al. (2003)

[a] Methods: SF, sap flow; EC, eddy covariance; M, models. NA: not available.

Table 5
Correlation analyses on relationships between monthly integrated *AOT*40, *SUM*0, *SUM*60, $AF_{st}0$, $AF_{st}1.0$ and $AF_{st}1.6$ from April 2013 to March 2015 (n = 24).

Indices	*AOT*40	*SUM*0	*SUM*60	$AF_{st}0$	$AF_{st}1.0$	$AF_{st}1.6$
*AOT*40	1	0.939**	0.992**	0.693**	0.675**	0.687**
*SUM*0		1	0.911**	0.716**	0.706**	0.690**
*SUM*60			1	0.690**	0.669**	0.687**
$AF_{st}0$				1	0.998**	0.995**
$AF_{st}1.0$					1	0.993**
$AF_{st}1.6$						1

*AOT*40: accumulated O_3 exposure over a threshold of 40 nmol mol^{-1} when photosynthetically active radiation (*PAR*) > 106 μmol m^{-2} s^{-1}. *SUM*0/*SUM*60: sum of hourly O_3 concentration ($[O_3]$) when $[O_3] \geq 0$/60 nmol mol^{-1}. $AF_{st}0/AF_{st}1.0/AF_{st}1.6$: accumulated O_3 flux over a threshold of 0/1.0/1.6 nmol m^{-2} s^{-1}.
** $p < 0.01$.

(Fares et al., 2010b). At the daily scale, although mean (daytime hours) $F_{st,O3}$ was linearly related to $[O_3]$ ($p < 0.01$), residuals of $F_{st,O3}$ were heterogeneous and proportional to $[O_3]$ (Fig. 6), implying large prediction uncertainties during periods of high $[O_3]$ (Grantz, 2014).

Integrated monthly, O_3 uptake doses were significantly correlated with the exposure doses, however, the correlation coefficients were systematically lower than those between different indices yet within the same dose category of either uptake or exposure (Table 5), which indicates the important role that $G_{st,O3}$ may play in determining stomatal O_3 uptake. Specifically, *AOT*40 in our experimental site reached the maximum in October in concurrence with a surge in daytime $[O_3]$ due to a transition from overcast/humid conditions in wet seasons to sunny/dry weather in dry seasons (Fig. 7a). However, mean $G_{st,O3}$ was reduced by high levels of *VPD* in October (1.73 kPa), and therefore $AF_{st}1.0$ peaked in July when both $G_{st,O3}$ and $[O_3]$ were moderately high (Fig. 7). Such discrepancy between the flux- and exposure-based metrics had also been observed in a Mediterranean evergreen forest (*Q. ilex*) in summer due to drought-induced stomatal closure, although at high $[O_3]$ (Fares et al., 2014). Likewise, the highest $[O_3]$ in springtime did not necessarily result in the highest O_3 uptake ($AF_{st}0$) in a temperate mixed deciduous and evergreen forest (*Q. serrata* and *I. pedunculosa*) because leaves of *Q. serrata* were not yet fully expanded and $G_{st,O3}$ was relatively low (Kitao et al., 2014). Across the 2 years of the experiment, $AF_{st}0$, $AF_{st}1.0$ (accumulated O_3 flux over a threshold of 1.0 nmol m^{-2} s^{-1}) and $AF_{st}1.6$ (accumulated O_3 flux over a threshold of 1.6 nmol m^{-2} s^{-1}) were on average 46.5%, 46.8% and 65.3% higher in wet seasons than in dry seasons, while *AOT*40, *SUM*0 and *SUM*60 were only 10.9%, 9.2% and 20.7% higher in wet seasons than in dry seasons (Table 6). These results illustrated the necessity and validity of using a flux-based rather than an exposure-based O_3 metrics in risk assessment (Paoletti and Manning, 2007).

4.3. Potential O_3 risk for S. superba

As growing seasons in our experimental site last all year round, and wet seasons typically span from April to September, which is consistent with the time duration used for defining critical O_3 levels for forest trees (UNECE, 2004), metrics for O_3 risk assessment were calculated for wet and dry seasons within each year, respectively. According to the exposure-based metrics, *AOT*40s (Table 6) in the present study were 1.0–1.6 times higher than the currently adopted critical level of 5 μmol mol^{-1} h for sensitive tree species in Europe (UNECE, 2004). *SUM*60s (Table 6) were 1.3–1.4 times of the US EPA proposed threshold of 25 μmol mol^{-1} ha^{-1} for vegetation protection in North America (US EPA, 1997). By contrast, in terms of the flux-based metrics, $AF_{st}1.6$ and $AF_{st}1.0$ (Table 6) were 2.9–5.5 and 4.6–7.7 times higher than the critical level of 4 mmol m^{-2}, which was set by being associated with a 4% reduction in tree growth per growing season (Karlsson et al., 2007; Mills et al., 2011). These results, on the one hand, reconfirm the differences between using flux- and exposure-based metrics in O_3 risk assessment (Paoletti and Manning, 2007); on the other hand, suggest that evergreen *S. superba* may potentially be stressed by ambient $[O_3]$ in our experimental site.

4.4. Limitations and prospects

However, it should be noted that the flux-based approach is still limited, because O_3 risk is not only determined by stomatal O_3 uptake, but also influenced by trees' O_3 sensitivity, which, in turn, depends on tree structure and metabolism, and varies with species, phenology, environment, season and time of the day (Dizengremel et al., 2008; Heath et al., 2009). Although much has been done to integrate O_3 flux and plants' sensitivity to establish an effective dose concept for more accurate O_3 risk evaluation (Grantz, 2014; Massman, 2004; Musselman et al., 2006; Tausz et al., 2007; Tuzet et al., 2011), no universally recognized metrics have so far been developed that could feasibly account for the inherent O_3 sensitivity. Alternatively, dendrochronological measurements provide a promising tool for isolating O_3 from other environmental factors and then anchoring it to the end point effects of tree growth reductions (McLaughlin et al., 2007; McLaughlin et al., 2002; McLaughlin et al., 2003). Analyses of stem increment data along O_3 exposure and/or flux gradients at regional and/or continental scales are thus have important implications for improved understanding and characterization of O_3 stress on trees. Secondly, the sap flow method used at the present study to derive stomatal O_3 flux is not free at present of limitations especially in view of the potential errors that might be involved, particularly under low *VPD* conditions (Ewers and Oren, 2000). It should be used in combination with stomatal conductance models and/or eddy covariance techniques for cross-calibrations. Lastly, the findings reported here were the outcome from only one evergreen tree species in a site that had not been affected by intense drought. For generalizations at a regional scale, quantifications of stomatal O_3 uptake for other native and nonnative tree species widely distributed in subtropical China under various soil moisture conditions are urgently required.

5. Conclusions

This study spanning all seasons over a 2-year period advanced our understanding about the canopy stomatal O_3 flux and uptake of a

Table 6
*AOT*40, *SUM*0, *SUM*60, $AF_{st}0$, $AF_{st}1.0$ and $AF_{st}1.6$ during wet and dry seasons from April 2013 to March 2015 (dry seasons: October–March; wet seasons: April–September).

Variables (units)	April 2013–March 2014			April 2014–March 2015		
	Wet season	Dry season	Whole year	Wet season	Dry season	Whole year
*AOT*40 (μmol mol^{-1} h)	12.85	11.60	24.45	11.07	9.96	21.03
*SUM*0 (μmol mol^{-1} h)	51.31	46.61	97.92	48.86	45.10	93.96
*SUM*60 (μmol mol^{-1} h)	20.23	17.46	37.69	18.19	14.38	32.57
$AF_{st}0$ (mmol m^{-2})	34.94	23.29	58.23	35.80	25.00	60.80
$AF_{st}1.0$ (mmol m^{-2})	34.23	22.47	56.70	34.62	24.44	59.06
$AF_{st}1.6$ (mmol m^{-2})	25.55	15.75	41.30	26.11	15.51	41.62

*AOT*40: accumulated O_3 exposure over a threshold of 40 nmol mol^{-1} when photosynthetically active radiation (*PAR*) > 106 μmol m^{-2} s^{-1}. *SUM*0/*SUM*60: sum of hourly O_3 concentration ($[O_3]$) when $[O_3] \geq 0$/60 nmol mol^{-1}. $AF_{st}0/AF_{st}1.0/AF_{st}1.6$: accumulated O_3 flux over a threshold of 0/1.0/1.6 nmol m^{-2} s^{-1}.

representative evergreen forest in subtropical China. Based on the findings shown in the Results and Discussion sections, and in correspondence to the hypotheses proposed in the Introduction section, we conclude that (1) $F_{st,O3}$ of *S. superba* was comparable to that reported in other tree species, regardless of leaf phenology (evergreen or deciduous) of the examined trees and the experimental methods that were adopted (sap flow, eddy covariance or models) (2) high $G_{st,O3}$ occurred asynchronously with high [O_3] at the diurnal and seasonal scales, therefore stomatal O_3 uptake was decoupled from O_3 exposure, and (3) the currently adopted *CL*s were notably exceeded, and *S. superba* may potentially be stressed by ambient O_3 in our experimental site. However, the exposure- and flux-based O_3 doses should be connected to some end point effects in tree growth for the ultimate confirmation of O_3 stress, and analyses on a wide range of tree species in subtropical China are imperatively needed to generalize our conclusions.

Acknowledgment

This study was supported by the National Natural Science Foundation of China (NO. 41275169), the Provincial Nature Science Foundation of Guangdong (NO. 2015A030310305 & NO. 2014A030313762) and the Doctoral Starting up Foundation of South China Botanical Garden, Chinese Academy of Sciences (NO. 201229). Any opinions, findings and conclusions or recommendations expressed in this material are those of the authors and do not necessarily reflect the views of funding sources.

References

Bell, D.M., Ward, E.J., Oishi, A.C., Oren, R., Flikkema, P.G., Clark, J.S., 2015. A state-space modeling approach to estimating canopy conductance and associated uncertainties from sap flux density data. Tree Physiol. 35, 792–802.

Bueker, P., Morrissey, T., Briolat, A., Falk, R., Simpson, D., Tuovinen, J.P., et al., 2012. DO_3SE modelling of soil moisture to determine ozone flux to forest trees. Atmos. Chem. Phys. 12, 5537–5562.

Campbell, G.S., Norman, J.M., 1998. An Introduction to Environmental Biophysics. Springer-Verlag, New York.

Clearwater, M.J., Meinzer, F.C., Andrade, J.L., Goldstein, G., Holbrook, N.M., 1999. Potential errors in measurement of nonuniform sap flow using heat dissipation probes. Tree Physiol. 19, 681–687.

Dizengremel, P., Le Thiec, D., Bagard, M., Jolivet, Y., 2008. Ozone risk assessment for plants: central role of metabolism-dependent changes in reducing power. Environ. Pollut. 156, 11–15.

Emberson, L.D., Ashmore, M.R., Cambridge, H.M., Simpson, D., Tuovinen, J.P., 2000. Modelling stomatal ozone flux across Europe. Environ. Pollut. 109, 403–413.

Ewers, B.E., Oren, R., 2000. Analyses of assumptions and errors in the calculation of stomatal conductance from sap flux measurements. Tree Physiol. 20, 579–589.

Fares, S., Goldstein, A., Loreto, F., 2010a. Determinants of ozone fluxes and metrics for ozone risk assessment in plants. J. Exp. Bot. 61, 629–633.

Fares, S., McKay, M., Holzinger, R., Goldstein, A.H., 2010b. Ozone fluxes in a *Pinus ponderosa* ecosystem are dominated by non-stomatal processes: evidence from long-term continuous measurements. Agr. Forest. Meteorol. 150, 420–431.

Fares, S., Matteucci, G., Mugnozza, G.S., Morani, A., Calfapietra, C., Salvatori, E., et al., 2013a. Testing of models of stomatal ozone fluxes with field measurements in a mixed Mediterranean forest. Atmos. Environ. 67, 242–251.

Fares, S., Vargas, R., Detto, M., Goldstein, A.H., Karlik, J., Paoletti, E., et al., 2013b. Tropospheric ozone reduces carbon assimilation in trees: estimates from analysis of continuous flux measurements. Glob. Chang. Biol. 19, 2427–2443.

Fares, S., Savi, F., Muller, J., Matteucci, G., Paoletti, E., 2014. Simultaneous measurements of above and below canopy ozone fluxes help partitioning ozone deposition between its various sinks in a Mediterranean Oak Forest. Agr. Forest. Meteorol. 198, 181–191.

Feng, Z., Tang, H., Uddling, J., Pleijel, H., Kobayashi, K., Zhu, J., et al., 2012. A stomatal ozone flux–response relationship to assess ozone-induced yield loss of winter wheat in subtropical China. Environ. Pollut. 164, 16–23.

Fowler, D., Amann, M., Anderson, R., Ashmore, M., Cox, P., Depledge, M., et al., 2008. Ground-level Ozone in the 21st Century: Future Trends, Impacts and Policy Implications. The Royal Society, London.

Granier, A., 1987. Evaluation of transpiration in a Douglas-fir stand by means of sap flow measurements. Tree Physiol. 3, 309–319.

Grantz, D.A., 2014. Diel trend in plant sensitivity to ozone: implications for exposure- and flux-based ozone metrics. Atmos. Environ. 98, 571–580.

Grulke, N.E., Preisler, H.K., Rose, C., Kirsch, J., Balduman, L., 2002. O_3 uptake and drought stress effects on carbon acquisition of ponderosa pine in natural stands. New Phytol. 154, 621–631.

Heath, R.L., Lefohn, A.S., Musselman, R.C., 2009. Temporal processes that contribute to nonlinearity in vegetation responses to ozone exposure and dose. Atmos. Environ. 43, 2919–2928.

Itahashi, S., Uno, I., Kim, S., 2013. Seasonal source contributions of tropospheric ozone over East Asia based on CMAQ-HDDM. Atmos. Environ. 70, 204–217.

Karlsson, P.E., Braun, S., Broadmeadow, M., Elvira, S., Emberson, L., Gimeno, B.S., et al., 2007. Risk assessments for forest trees: the performance of the ozone flux versus the AOT concepts. Environ. Pollut. 146, 608–616.

Kinose, Y., Azuchi, F., Uehara, Y., Kanomata, T., Kobayashi, A., Yamaguchi, M., et al., 2014. Modeling of stomatal conductance to estimate stomatal ozone uptake by *Fagus crenata*, *Quercus serrata*, *Quercus mongolica* var. *crispula* and *Betula platyphylla*. Environ. Pollut. 194, 235–245.

Kitao, M., Komatsu, M., Hoshika, Y., Yazaki, K., Yoshimura, K., Fujii, S., et al., 2014. Seasonal ozone uptake by a warm-temperate mixed deciduous and evergreen broadleaf forest in western Japan estimated by the Penman–Monteith approach combined with a photosynthesis-dependent stomatal model. Environ. Pollut. 184, 457–463.

Laisk, A., Kull, O., Moldau, H., 1989. Ozone concentration in leaf intercellular air spaces is close to zero. Plant Physiol. 90, 1163–1167.

Lee, J.-B., Cha, J.-S., Hong, S.-C., Choi, J.-Y., Myoung, J.-S., Park, R.J., et al., 2015. Projections of summertime ozone concentration over East Asia under multiple IPCC SRES emission scenarios. Atmos. Environ. 106, 335–346.

Logan, J.A., Staehelin, J., Megretskaia, I.A., Cammas, J.P., Thouret, V., Claude, H., et al., 2012. Changes in ozone over Europe: analysis of ozone measurements from sondes, regular aircraft (MOZAIC) and alpine surface sites. J. Geophys. Res.-Atmos. 117, 23.

Massman, W.J., 2004. Toward an ozone standard to protect vegetation based on effective dose: a review of deposition resistances and a possible metric. Atmos. Environ. 38, 2323–2337.

Matyssek, R., Wieser, G., Nunn, A.J., Kozovits, A.R., Reiter, I.M., Heerdt, C., et al., 2004. Comparison between AOT40 and ozone uptake in forest trees of different species, age and site conditions. Atmos. Environ. 38, 2271–2281.

Matyssek, R., Sandermann, H., Wieser, G., Booker, F., Cieslik, S., Musselman, R., et al., 2008. The challenge of making ozone risk assessment for forest trees more mechanistic. Environ. Pollut. 156, 567–582.

Matyssek, R., Wieser, G., Ceulemans, R., Rennenberg, H., Pretzsch, H., Haberer, K., et al., 2010. Enhanced ozone strongly reduces carbon sink strength of adult beech (*Fagus sylvatica*)—resume from the free-air fumigation study at Kranzberg Forest. Environ. Pollut. 158, 2527–2532.

Matyssek, R., Baumgarten, M., Hummel, U., Haeberle, K.H., Kitao, M., Wieser, G., 2015. Canopy-level stomatal narrowing in adult *Fagus sylvatica* under O_3 stress — means of preventing enhanced O_3 uptake under high O_3 exposure? Environ. Pollut. 196, 518–526.

McLaughlin, S.B., Shortle, W.C., Smith, K.T., 2002. Dendroecological applications in air pollution and environmental chemistry: research needs. Dendrochronologia 20, 133–157.

McLaughlin, S.B., Wullschleger, S.D., Nosal, M., 2003. Diurnal and seasonal changes in stem increment and water use by yellow poplar trees in response to environmental stress. Tree Physiol. 23, 1125–1136.

McLaughlin, S.B., Nosal, M., Wullschleger, S.D., Sun, G., 2007. Interactive effects of ozone and climate on tree growth and water use in a southern Appalachian forest in the USA. New Phytol. 174, 109–124.

Mei, T.T., Zhao, P., Wang, Q., Cai, X.A., Yu, M.H., Zhu, L.W., et al., 2010. Effects of tree diameter at breast height and soil moisture on transpiration of *Schima superba* based on sap flow pattern and normalization. The Journal of Applied Ecology 21, 2457–2464.

Meinzer, F.C., Goldstein, G., Andrade, J.L., 2001. Regulation of water flux through tropical forest canopy trees: do universal rules apply? Tree Physiol. 21, 19–26.

Mills, G., Pleijel, H., Büker, P., Braun, S., Emberson, L.D., Harmens, H., Hayes, F., Simpson, D., Grünhage, L., Karlsson, P.E., Danielsson, H., Bermejo, V., Gonzalez Fernandez, I., 2010. Vegetation. Revision undertaken in Summer 2010 to include new flux-based critical levels and response functions for ozone. Mapping Manual 2004. International Cooperative Programme on Effects of Air Pollution on Natural Vegetation and Crops.

Mills, G., Pleijel, H., Braun, S., Bueker, P., Bermejo, V., Calvo, E., et al., 2011. New stomatal flux-based critical levels for ozone effects on vegetation. Atmos. Environ. 45, 5064–5068.

Montheith, J.M.L., Unsworth, M.H., 1990. Principles of Environmental Physics. Edward Arnold, London.

Musselman, R.C., Lefohn, A.S., Massman, W.J., Heath, R.L., 2006. A critical review and analysis of the use of exposure- and flux-based ozone indices for predicting vegetation effects. Atmos. Environ. 40, 1869–1888.

Nunn, A.J., Wieser, G., Metzger, U., Loew, M., Wipfler, P., Haeberle, K.-H., et al., 2008. Exemplifying whole-plant ozone uptake in adult forest trees of contrasting species and site condition. Environ. Pollut. 151, 678–679.

Nunn, A.J., Cieslik, S., Metzger, U., Wieser, G., Matyssek, R., 2010. Combining sap flow and eddy covariance approaches to derive stomatal and non-stomatal O_3 fluxes in a forest stand. Environ. Pollut. 158, 2014–2022.

Oishi, A.C., Oren, R., Stoy, P.C., 2008. Estimating components of forest evapotranspiration: a footprint approach for scaling sap flux measurements. Agr. Forest. Meteorol. 148, 1719–1732.

Oren, R., Sperry, J.S., Katul, G.G., Pataki, D.E., Ewers, B.E., Phillips, N., et al., 1999. Survey and synthesis of intra- and interspecific variation in stomatal sensitivity to vapour pressure deficit. Plant Cell Environ. 22, 1515–1526.

Paoletti, E., Manning, W.J., 2007. Toward a biologically significant and usable standard for ozone that will also protect plants. Environ. Pollut. 150, 85–95.

Phillips, N., Oren, R., 1998. A comparison of daily representations of canopy conductance based on two conditional time-averaging methods and the dependence of daily conductance on environmental factors. Annales Des Sciences Forestieres 55, 217–235.

Seok, B., Helmig, D., Ganzeveld, L., Williams, M.W., Vogel, C.S., 2013. Dynamics of nitrogen oxides and ozone above and within a mixed hardwood forest in northern Michigan. Atmos. Chem. Phys. 13, 7301–7320.

Sitch, S., Cox, P.M., Collins, W.J., Huntingford, C., 2007. Indirect radiative forcing of climate change through ozone effects on the land-carbon sink. Nature 448, 791–794.
Tang, H., Takigawa, M., Liu, G., Zhu, J., Kobayashi, K., 2013. A projection of ozone-induced wheat production loss in China and India for the years 2000 and 2020 with exposure-based and flux-based approaches. Glob. Chang. Biol. 19, 2739–2752.
Tang, H., Pang, J., Zhang, G., Takigawa, M., Liu, G., Zhu, J., et al., 2014. Mapping ozone risks for rice in China for years 2000 and 2020 with flux-based and exposure-based doses. Atmos. Environ. 86, 74–83.
Tausz, M., Grulke, N.E., Wieser, G., 2007. Defense and avoidance of ozone under global change. Environ. Pollut. 147, 525–531.
Tuzet, A., Perrier, A., Loubet, B., Cellier, P., 2011. Modelling ozone deposition fluxes: the relative roles of deposition and detoxification processes. Agr. Forest. Meteorol. 151, 480–492.
Uddling, J., Hogg, A.J., Teclaw, R.M., Carroll, M.A., Ellsworth, D.S., 2010. Stomatal uptake of O-3 in aspen and aspen-birch forests under free-air CO2 and O-3 enrichment. Environ. Pollut. 158, 2023–2031.
UNECE, 2004. Manual on Methodologies and Criteria for Modeling and Mapping Critical Loads & Levels and Air Pollution Effects, Risk and Trends.
US EPA, 1997. National ambient air quality standards for ozone: final rule. Fed. Regist. 62, 38855–38896.
US EPA. Integrated Science Assessment of Ozone and Related Photochemical Oxidants (Final Report). In: Agency, U.S.E.P. (Ed.), 2013.
van Goethem, T.M.W.J., Azevedo, L.B., van Zelm, R., Hayes, F., Ashmore, M.R., Huijbregts, M.A.J., 2013. Plant species sensitivity distributions for ozone exposure. Environ. Pollut. 178, 1–6.
Wang, H., Zhou, W., Wang, X., Gao, F., Zheng, H., Tong, L., et al., 2012. Ozone uptake by adult urban trees based on sap flow measurement. Environ. Pollut. 162, 275–286.
Wieser, G., Matyssek, R., Kostner, B., Oberhuber, W., 2003. Quantifying ozone uptake at the canopy level of spruce, pine and larch trees at the alpine timberline: an approach based on sap flow measurement. Environ. Pollut. 126, 5–8.
Wieser, G., Luis, V.C., Cuevas, E., 2006. Quantification of ozone uptake at the stand level in a *Pinus canariensis* forest in Tenerife, Canary Islands: an approach based on sap flow measurements. Environ. Pollut. 140, 383–386.
Wittig, V.E., Ainsworth, E.A., Naidu, S.L., Karnosky, D.F., Long, S.P., 2009. Quantifying the impact of current and future tropospheric ozone on tree biomass, growth, physiology and biochemistry: a quantitative meta-analysis. Glob. Chang. Biol. 15, 396–424.
Zhao, X.-W., Zhao, P., Zhu, L.-W., Ni, G.-Y., Zeng, X.-P., Niu, J.-F., 2013. Seasonal dynamics of night-time stem water recharge of *Schima superba* and its relation to tree architecture and leaf biomass. Chinese Journal of Plant Ecology 37, 239–247.
Zhou, C.-m., Zhao, P., G-y, N., Wang, Q., X-p, Z., Zhu, L.-w., et al., 2012. Water recharge through nighttime stem sap flow of *Schima superba* in Guangzhou region of Guangdong Province, South China: affecting factors and contribution to transpiration. The Journal of Applied Ecology 23, 1751–1757.
Zhu, L.W., Zhao, P., Cai, X.A., Zeng, X.P., Ni, G.Y., Zhang, J.Y., et al., 2012. Effects of sap velocity on the daytime increase of stem CO_2 efflux from stems of *Schima superba* trees. Trees-Structure and Function 26, 535–542.